NANO · MICRO small
www.small-journal.com

Ultrasensitive and Selective Protein Recognition with Nanobody-Functionalized Synthetic Nanopores

*Ivana Duznovic, Alexander Gräwe, Wadim Weber, Lena K. Müller, Mubarak Ali, Wolfgang Ensinger, Alesia Tietze, and Viktor Stein**

The development of flexible and reconfigurable sensors that can be readily tailored toward different molecular analytes constitutes a key goal and formidable challenge in biosensing. In this regard, synthetic nanopores have emerged as potent physical transducers to convert molecular interactions into electrical signals. Yet, systematic strategies to functionalize their surfaces with receptor proteins for the selective detection of molecular analytes remain scarce. Addressing these limitations, a general strategy is presented to immobilize nanobodies in a directional fashion onto the surface of track-etched nanopores exploiting copper-free click reactions and site-specific protein conjugation systems. The functional immobilization of three different nanobodies is demonstrated in ligand binding experiments with green fluorescent protein, mCherry, and α-amylase (α-Amy) serving as molecular analytes. Ligand binding is resolved using a combination of optical and electrical recordings displaying quantitative dose–response curves. Furthermore, a change in surface charge density is identified as the predominant molecular factor that underlies quantitative dose–responses for the three different protein analytes in nanoconfined geometries. The devised strategy should pave the way for the systematic functionalization of nanopore surfaces with biological receptors and their ability to detect a variety of analytes for diagnostic purposes.

1. Introduction

The development of generally applicable sensing modulaties that can be readily configured to detect any molecular analyte constitutes a key goal in biosensing.[1] Applications are numerous and range from detecting clinically-relevant biomarkers in complex biological fluids to monitoring pollutants in the environment.[2] From a technical point of view, one of the key challenges concerns the conversion of a molecular interaction into a measureable, quantitative, and physical read-out.

In this regard, track-etched nanopores in polymer membranes have emerged as a versatile class of physical transducers. Crucially, depending on the chemical and biological functionalization, track-etched nanopores can be transformed into highly specific biosensors that are capable of resolving molecular interactions through altered electrical signals across the membrane. Mechanisms of sensing include both stochastic (i.e., resistive pulse sensing) and steady-state approaches (i.e., modulation in ion current rectification characteristics).[3,4] Key considerations that determine the responsiveness of receptor-modified nanopores toward a desired analyte concerns their material, size, geometry, and surface properties.[3] In this regard, several label-free sensors have been developed exploiting small molecules[5–7] or DNA aptamers[8,9] as receptors to detect a range of different analytes including metal ions,[5,10] low molecular weight ligands,[6,8,11] nucleic acids,[12] or proteins.[7,9,13,14] In contrast, the use of receptor proteins has been limited to a few model interactions, in particular, conventional antibody-antigen combinations and streptavidin-biotin.[15,16]

Dr. I. Duznovic, Dr. M. Ali, Prof. W. Ensinger
Technische Universität Darmstadt
Fachbereich Material- und Geowissenschaften
Fachgebiet Materialanalytik
Alarich-Weiss-Str. 2, D-64287 Darmstadt, Germany
Dr. A. Gräwe, Dr. W. Weber, Prof. V. Stein
Department of Biology
TU Darmstadt
64287 Darmstadt, Germany
E-mail: stein@bio.tu-darmstadt.de

The ORCID identification number(s) for the author(s) of this article can be found under https://doi.org/10.1002/smll.202101066.

DOI: 10.1002/smll.202101066

Dr. A. Gräwe, Dr. W. Weber, Prof. V. Stein
Centre for Synthetic Biology
TU Darmstadt
64283 Darmstadt, Germany
Dr. L. K. Müller, Dr. A. Tietze
Technische Universität Darmstadt
Clemens-Schöpf Institute of Organic Chemistry and Biochemistry
Alarich-Weiss Str. 4, 64287 Darmstadt, Germany
Dr. M. Ali
GSI Helmholtz-Center for Heavy Ion Research
Planckstr. 1, D-64291 Darmstadt, Germany
Dr. A. Tietze
University of Gothenburg
Department of Chemistry and Molecular Biology
Wallenberg Centre for Molecular and Translational Medicine
Kemigården 4, Göteborg 412 96, Sweden

Addressing these limitations, a modular approach is devised to functionalize track-etched nanopores with nanobodies (Nbs). Nbs comprise a versatile class of single-chain antibodies that originate from the immune system of alpacas, and find increasing use in many biotechnological applications.[17,18] Compared to antibodies, Nbs promise several key advantages in the context of a nanopore sensor: First, Nbs consist of a single 15 kDa immunoglobulin domain that is one-tenth the size compared to conventional antibodies. Accordingly, any binding event will have a greater effect in relation to the receptor and thus proportionately generate a stronger change in the electrical response. Second, Nbs can be readily expressed in *Escherichia coli* in high-yield independent of mammalian cell lines which is time consuming and requires specialist expertise.[17] Importantly, a recombinant route greatly facilitates further modifications to a receptor protein such as the introduction of a site-specific protein conjugation tag, which ensures consistent spatial arrangements irrespective of the underlying binding specificity as the orientation of the N- and C-termini is preserved in the context of a nanobody. In comparison, the immobilization of antibodies is limited to non-specific chemical conjugation methods, for instance, via the NH_2 group of lysine residues to surface activated COOH groups, which only provides little control over the orientation with potentially detrimental effects, for instance, if the binding site is occluded. Fourth, Nbs can be generated by immunization and are continuously being developed for a range of applications in molecular and cell biology yielding an ever increasing repertoire of recombinant binders.[18] Crucially, access to Nbs is greatly facilitated by publically available sequences and high-resolution structural information. Finally, the specificity, the affinity and other key functional properties such as the thermodynamic stability can be optimized and fine-tuned using a variety of genetic screening and selection systems.[18]

In this work, Nbs are assessed and developed as generic receptor modules to sense molecular analytes in the context of track-etched nanopores. To this end, nanopores are first fabricated in heavy ion irradiated polyethylene terephthalate (PET) membranes based on the track-etching technique. The resulting COOH-moieties on the nanopore surface are then functionalized with three different Nbs that specifically bind green fluorescent protein (GFP),[19] mCherry (mCh)[20] and α-amylase (α-Amy).[21] The immobilization of Nbs is achieved in a covalent and directed fashion based on the combined action of Sortase A[22,23] and the SpyTag/Catcher system.[24] Furthermore, ligand binding is successfully confirmed by electrical and optical means demonstrating quantitative dose–response curves for the three different analytes in nanoconfined geometries.

2. Results

2.1. Molecular Design Considerations

Toward the development of a reconfigurable biosensor platform, a modular strategy was devised to immobilize Nbs on the surface of track-etched membranes (**Figure 1**). To facilitate electrical recordings, nanopores generally featured a conical geometry hypothesizing that the cone tip opening exhibits a more responsive electrical signal when an analyte molecule bound to its cognate nanobody.[3,25] Note that single-pore membranes were analyzed by changes in electrical signals in the form of current–voltage (*I–V*) curves (**Figures 2**,**3**) while multipore membranes were characterized by optical means, that is, modulation in fluorescent signals (**Figures 4**,**5**). A summary of membranes and their experimental characterization is provided (Figures S1,S2, Tables S1–S3, Supporting Information).

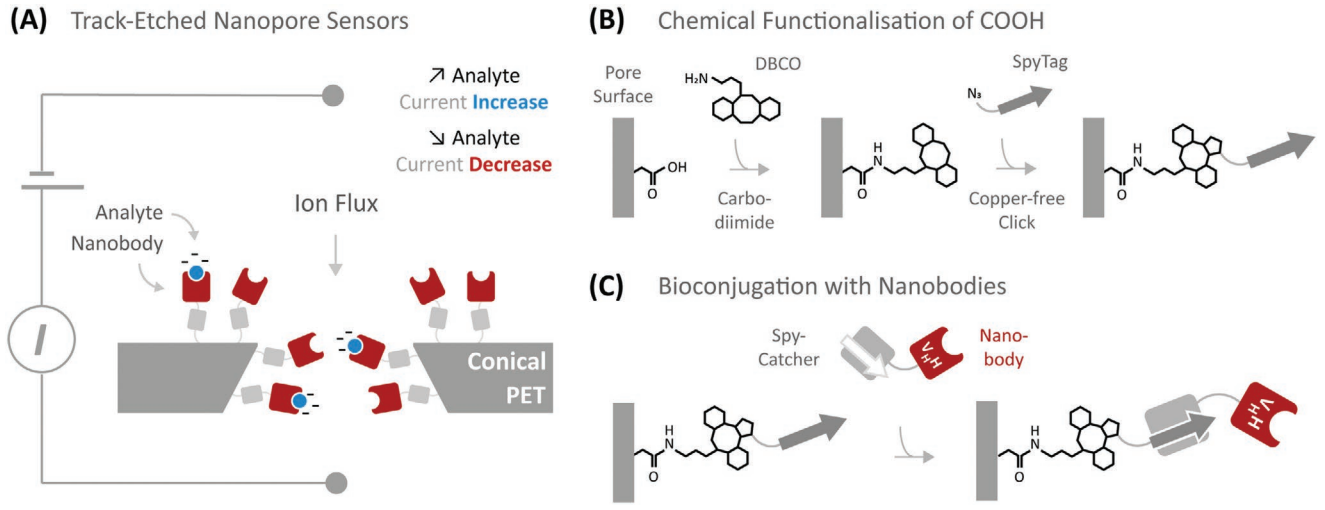

Figure 1. A modular strategy for the oriented immobilization of nanobodies on the surface of track-etched nanopores. A) The binding of protein analytes to their cognate nanobodies is experimentally resolved through altered current–voltage (*I–V*) curves across the membrane; negative charges are indicated reflecting the net negative charge of the protein analytes GFP, mCherry, and α-Amy tested in this study; B) scheme representing the attachment of dibenzocyclooctyne-amine (DBCO) to surface-exposed COOH-groups. Functionalization with DBCO subsequently enables the attachment of an azide-terminated SpyTag-tether via Cu^{I}-free click chemistry; C) nanobodies are then conjugated to the nanopore surface via SpyTag-SpyCatcher-mediated covalent interactions. Use of a site-specific protein conjugation tag enables the orientated immobilization inside the nanopore ensuring the antigen binding site points away from the nanopore surface into the nanopore lumen.

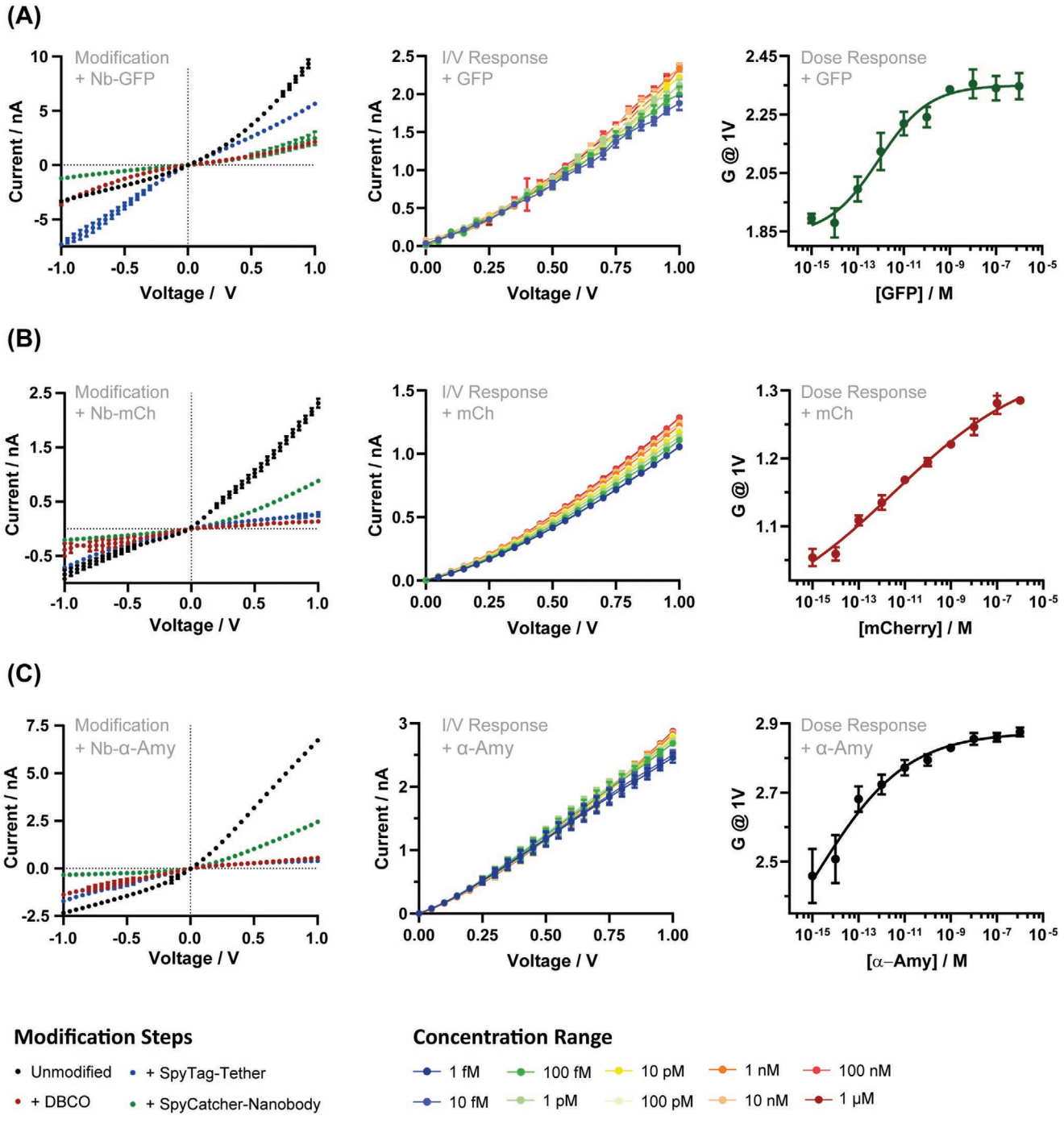

Figure 2. Summary of *I–V* recordings monitoring the functionalization of single conical nanopores with A) Nb^{GFP}, B) Nb^{mCh} and C) $Nb^{\alpha\text{-}Amy}$, and concentration-dependent changes following interaction with their cognate ligands in nanoconfined geometries. Left: Step-wise functionalization of single PET nanopores with i) hydrophobic DBCO, ii) positively charged SpyTag-tether and iii) negatively charged SpyCatcher-Nb; Middle: Summary of I/V recordings for increasing concentrations of the protein analyte. The current increases in response to increasing concentrations of GFP, mCherry, and α-amylase and is associated with increasing negative charge density of the ligand analytes. Right: Summary of ligand titrations displaying quantitative dose–response curves. Error bars derive from three periods of triangular voltage recordings on a single-pore membrane. The dimensions of single nanopores were calculated according to established protocols[25] (Tip/Base in nm): Nb^{GFP} 26/550; Nb^{mCh} 45/650; $Nb^{\alpha\text{-}Amy}$ 38/580.

Functionalization of the nanopore surface was achieved in three consecutive steps exploiting copper-free click reactions and the combined action of Sortase A[23,26] and the site-specific SpyTag/Catcher protein conjugation system (Figure 1A).[24,27,28] Briefly, the dibenzocyclooctyne-amine (DBCO) was first covalently attached to the COOH-groups on the nanopore surface via carbodiimide coupling chemistry.[5] Second, the azide-terminated SpyTag002-tether peptide (SpyTag-tether) was linked to the DBCO

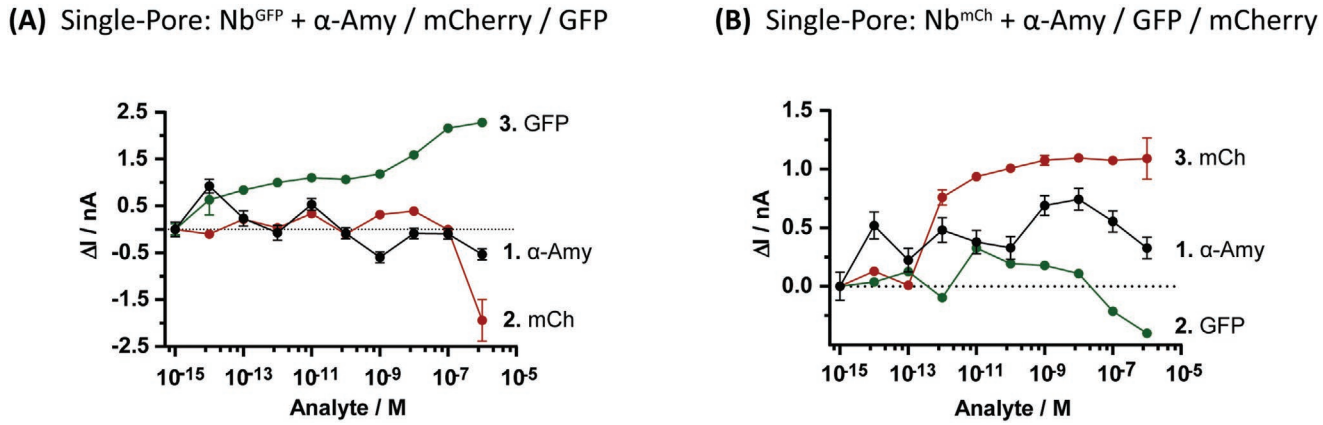

Figure 3. Summary of *I–V* recordings of single conical nanopores modified separately with A) Nb^{GFP} and B) Nb^{mCh} and treatment with different ligands. No increase in the signal is observed upon addition of non-cognate ligands albeit a deterioration in sensitivity for the cognate ligand. The order of ligands that were applied to the membrane is indicated. Error bars derive from three periods of triangular voltage recordings on a single-pore membrane. Nanopore dimensions of single membranes (Tip/Base in nm): Nb^{GFP} 51/680; Nb^{mCh} 42/510.

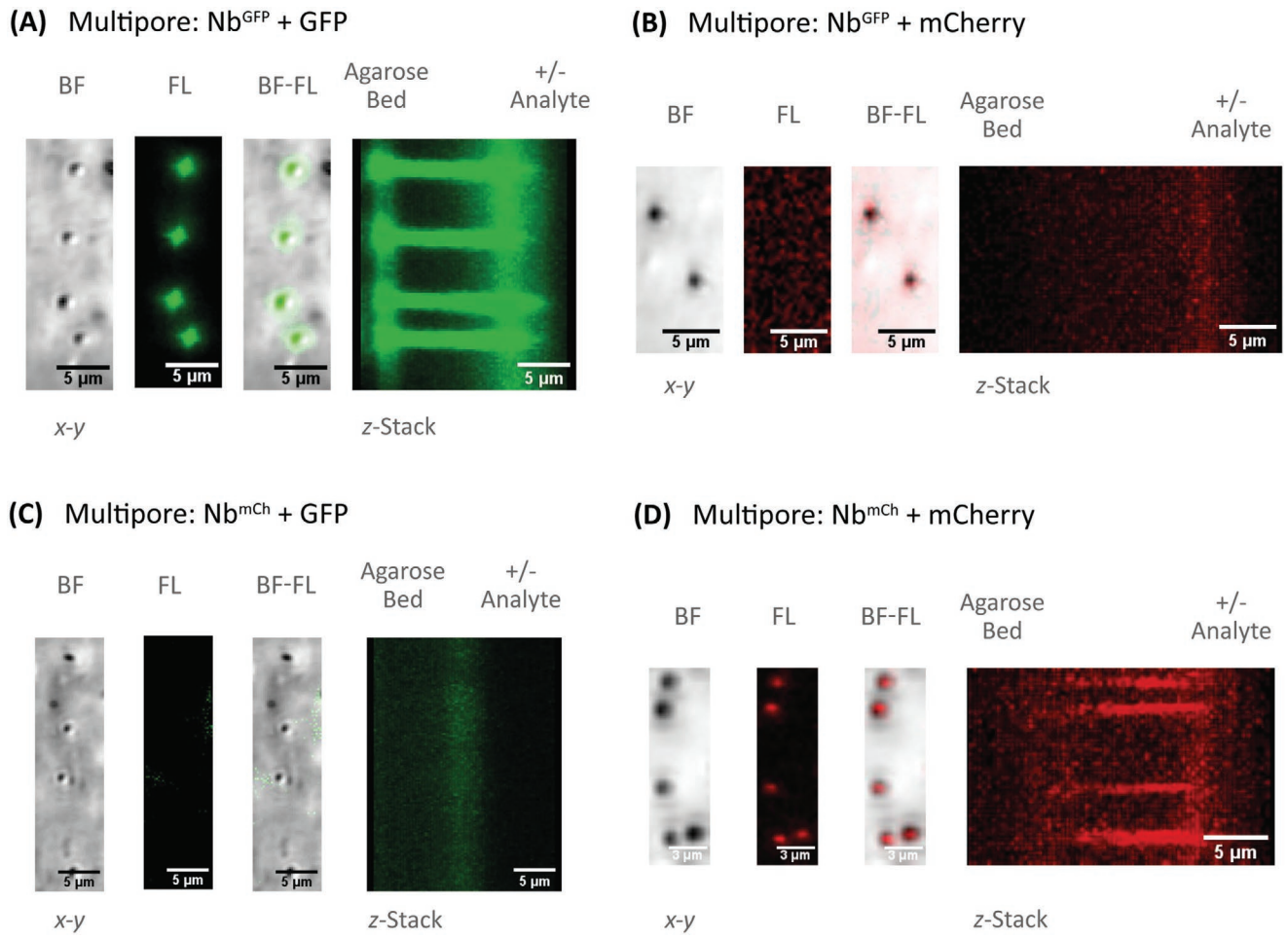

Figure 4. Summary of CLSM analysis of nanobody-ligand interactions on multiporous membranes featuring cylindrical nanopores: Membranes were either functionalized with A,B) Nb^{GFP} or C,D) Nb^{mCh} and then treated with GFP and mCherry ligand as indicated. Strong fluorescent signals reflecting the cylindrical shape of the nanopore are only observed for cognate nanobody–ligand interactions. Cylindrical nanopores generally featured a diameter of 200 nm. BF: Brightfield image; FL: Fluorescent image; BF-BL: Brightfield-fluorescent image combined; Agarose Bed denotes the side of the membrane facing the agarose bed; +/– Analyte denotes the side of the membrane the analyte is added and subsequently washed out.

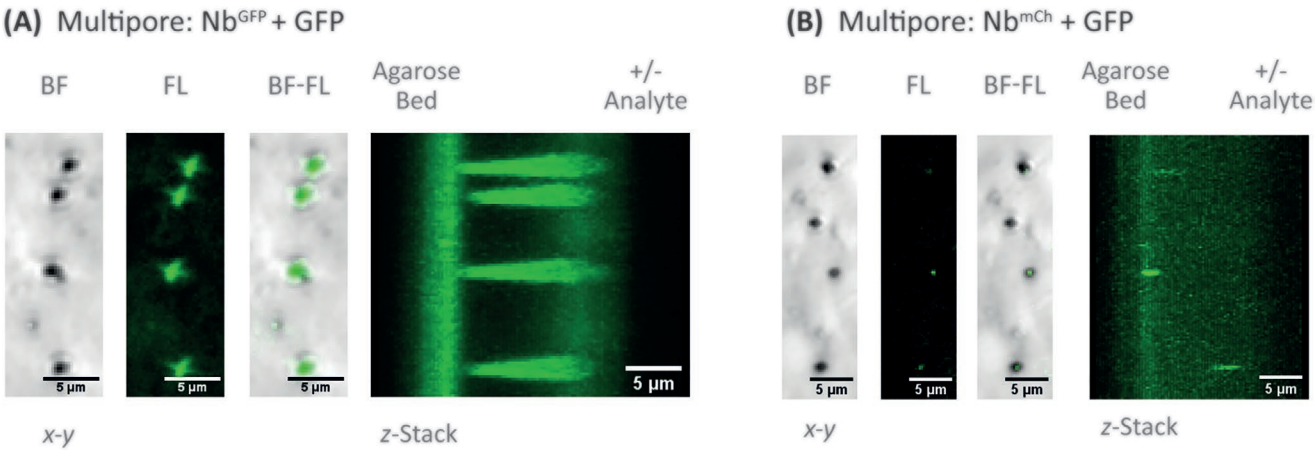

Figure 5. Summary of CLSM analysis of nanobody–ligand interactions on multiporous membranes featuring conical nanopores: Multipore membranes were functionalized with Nb^{GFP} and then either treated with A) GFP or B) mCherry as indicated. Strong fluorescent signals reflecting the conical shape of the nanopore were only observed for Nb^{GFP}, but not Nb^{mCh}-functionalized nanopores; BF: Brightfield image; FL: Fluorescent image; BF-BL: Brightfield-fluorescent image combined; Agarose Bed denotes the side of the membrane facing the agarose bed; +/− Analyte denotes the side of the membrane the analyte is added and subsequently washed out. Nanopore dimensions of multipore membranes (Tip/Base in nm): Nb^{GFP} 33/490; Nb^{mCh} 28/425.

moiety via copper-free strain-promoted azide-alkinyl cycloaddition (Figure 1B). Note, the SpyTag-tether could be recombinantly produced and purified as a maltose binding protein (MBP) fusion protein in *E. coli* before the azide moiety was introduced by the Ca^{2+}-dependent Sortase A5M.[23,26] The MBP-tag was subsequently cleaved off by tobacco etch virus (TEV) protease and the SpyTag-tether attached to the nanopore surface via the cyclooctene group of DBCO. Third, individual SpyCatcher002-nanobody (SpyCatcher-Nb) modules were covalently conjugated to the SpyTag-tether on the nanopore surface (Figure 1C). Note, considering the C-terminus of the nanobody was fused to the N-terminus of the SpyCatcher, the ligand binding site of the nanobody generally points away from the surface into the lumen of the nanopore and thus ensures steric access to the ligand.

2.2. *I–V* Recordings with Single-Pore Membranes

To demonstrate the utility of Nb-functionalized nanopores in the context of an electrical biosensor, three different Nbs Nb^{GFP}, Nb^{mCh}, and $Nb^{\alpha\text{-Amy}}$ that could specifically bind GFP, mCh, and α-Amy were individually immobilized onto the surface of single conical nanopores. The success of nanopore functionalization was generally monitored via changes in the *I–V* recordings (Figure 2). It is well known that in case of conical nanopores, minor changes either in the surface charge or effective diameter of the nanopore can be directly visualized from the modulation of ion transport across the membrane. Importantly, while the ≈26–45 nm diameter of the tip directly impacts the conductivity of the nanopore and its responsiveness upon covalent conjugation, the trend regarding rectification remains equivalent across all nanopores during their functionalization process (Figure 2). Specifically, the attachment of uncharged, hydrophobic DBCO moieties on the pore surface led to a lower ionic conductance with an almost linear *I–V* curve. Upon conjugation of the positively charged SpyTag-tether with an estimated net charge of +5.2 at pH 7.4 (Table S4, Supporting Information) to DBCO, the nanopore becomes anion-selective as can be seen from the inversion of current rectification. In contrast, conjugation of SpyCatcher-Nb^{GFP} and SpyCatcher-Nb^{mCh} with an estimated net charge of −9.8 to −7.8 at pH 7.4 (Table S4, Supporting Information) resulted in a cation selective nanopore as is evidenced from the rectification behavior.

In a subsequent step, the capacity of Nbs to resolve binding interactions inside nanopores was examined. To this end, the concentration of the cognate analyte, that is, GFP and mCh was gradually increased from 10^{-15} to 10^{-6} M in PBS buffer (pH 7.4) that has been supplemented with an additional 100 mM KCl (Figure 2A,B). Notably, the addition of GFP and mCh caused a quantitative increase in the current across the membrane that could be recorded over multiple orders of magnitude. This can be attributed to a net negative charge of −6.1 and −7.5 for GFP and mCh at pH 7.4 (Table S4, Supporting Information) resulting in higher negative charge densities on the pore surface which in turn enhanced the cationic movement across the membrane. Furthermore, concentration-dependent increases in the current could be resolved 2 to 3 orders below the dissociation constants (K_D) of the Nb^{GFP}–GFP and Nb^{mCh}–mCh interactions observed in solution (K_D = ≈1.4 nM for Nb^{GFP} ;[19] K_D = ≈0.4 nM for Nb^{mCh},[20] Clone ID: LaM-4). Similar gains in the sensitivity were previously observed for a Cu^{II}-specific sensor and could be attributed to confinement effects as receptors immobilized at the nanopore tip are present at high effective concentrations and therefore able to confer a high responsiveness at low analyte concentrations.[5]

To demonstrate the versatility of the approach further, another single conical nanopore membrane was functionalized with a nanobody specific for α-Amy.[21] Notably, α-Amy carries diagnostic relevance as it constitutes a biomarker for acute pancreatitis.[29] Analogous to Nb^{GFP} and Nb^{mCh}-functionalized membranes, the modification with SpyCatcher-$Nb^{\alpha Am}$ caused cation selective signal rectification while the addition of α-Amy triggered a quantitative increase in the current that could be resolved at substantially lower concentrations compared to the K_D observed in solution (Figure 2C).[21]

Furthermore, electrical recordings triggered no increase in the current following increasing concentrations of non-cognate

analytes. However, the performance of the membrane deteriorated when GFP and mCh were only applied to the membrane after the non-cognate ligands (Figure 3A,B). One explanation could be that repeated application of high-voltages up to 1 V either fully or partially unfolded proteins, which has previously been observed for small globular signaling proteins passing through solid state nanopores.[30] Such voltage inflicted damage may manifest itself in a gradual and cumulative fashion as proteins may undergo iterative cycles of partial unfolding and refolding upon exposure to an electrical field.[31,32] To what extent such damage affects the performance of a nanopore sensor in practice will ultimately depend on individual biophysical parameters, in particular, the thermodynamic stability and the capacity of a protein to refold following partial denaturation.

2.3. Optical Imaging with Multipore Membranes

Moreover, the binding specificity of Nbs immobilized onto the pore surface was analyzed in a semi-quantitative fashion by confocal laser scanning microscopy (CLSM) using multipore membranes featuring cylindrical (Figure 4) and conical nanopores (Figure 5). Crucially, CLSM experiments provide unique insights into the spatial functionalization of synthetic nanopores. In particular, one can assess to what extent the binding of an analyte is limited to the nanopore or whether it occurs on the membrane surface, too. To facilitate the identification of individual nanopores and enhance their wettability, cylindrical nanopores with a diameter of 200 nm and a density of 10^7 pores per cm^2 membrane were used. To this end, membranes that have been functionalized with either Nb^{GFP} or Nb^{mCh} were mounted on coverslips coated with 0.5% agarose while GFP and mCh were added and incubated for another 30 min. The membranes were then washed twice with PBS before being analyzed by CLSM via top view and scanning mode. Crucially, strong fluorescent signals were only observed for cognate interactions, demonstrating that Nbs retained their specifity upon immobilization in confined geometries (Figure 4A,D). Conversely, only marginal fluorescent spots were observed for non-cognate interactions (Figure 4B,C). Furthermore, fluorescence is generally more concentrated inside the nanopore compared to the surface of the membrane which is particularly evident for mCh (Figure 4D). This provides additional evidence that the analyte preferably binds inside the nanopore which can be rationalized by confinement effects and is conclusive with the high-sensitivity observed in electrical recordings. In addition, binding might be enhanced by a greater amount of COOH groups that are generated as a result of the ion track etching procedure, and thus enable the immobilization of a greater amount of Nbs.

Finally, the specificity of nanobody–ligand interactions was analyzed in the context of conical multipore membranes (Figure 5). Similar to cylindrical multipore membranes, CLSM measurements demonstrate that nanobody–ligand interactions are specific inside nanopores as a green fluorescent signal was only observed for nanopores functionalized with Nb^{GFP} (Figure 5A) but not Nb^{mCh} (Figure 5B). Compared to cylindrical nanopores, membranes with conical nanopores feature more fluorescent signal at the tip side facing the agarose bed. This can be attributed to a narrower diameter of the nanotip slowing down the diffusion and ability to wash out GFP analyte at the base side.

3. Discussion

Track-etched polymer membranes carry great potential in biosensing but the scope of receptor proteins that have been successfully immobilized in the context of a nanopore sensor remains limited. Arguably, conventional antibodies have been preferred because of their widespread commercial availability which facilitates access to non-specialists. Yet, complex expression protocols based on mammalian cell lines generally prohibit their facile modification and adaptation to the functional requirements of a nanopore sensor by recombinant means.

Addressing these limitations, a modular approach is devised that combines the exquisite sensitivity of track-etched nanopores with the specificity and versatility of Nbs. The approach is technically simple as Nbs are directly conjugated to the surface of track-etched PET membranes based on the combined action of Sortase A[23] and SpyCatcher.[24,27,28] Crucially, the capacity of Nbs to bind their cognate protein ligand was preserved inside the nanopore. Notably, highly sensitive and quantitative dose–response curves could be demonstrated for three different protein analytes GFP, mCh, and α-Amy. Increasing currents upon ligand binding for all three protein analytes employed in this study suggest that highly charged ligands generally enhance the rectified ion flux across the nanopore. Conversely, size plays a secondary role in this particular configuration as no decrease in the current is observed across the nanopore despite comparable dimensions of the ligand-receptor complex and the diameter of the nanopore tip that could potentially block the pore.

In addition, dose–response curves turn out ultrasensitive over at least three orders of magnitude that can resolve binding interactions below the K_D for the individual interactions observed in solution. Such enhanced sensitivity can be readily attributed to confinement effects that are associated with the conical geometry of the nanopores[5] and have also been observed for other chemical and biophysical parameters in nanoporous materials.[33] This means, a comparatively small nanopore opening that is tens of nanometers in diameter confines receptors in a disproportionately small volume to enhance molecular interactions. Second, a high aspect ratio provides a long sensing channel on which binding of the cognate ligand can exert a sensitive change in the electrical readout. The high responsiveness could also be harnessed in the analysis of more complex samples, for instance, affording dilution in standardized buffers and pre-processing the sample in a microfluidic device.

In a complementary experimental approach, binding interactions were analyzed by CLSM which provides further semi-quantitative insight into the spatial functionalization of track-etched nanopore sensors. Notably, fluorescent signals associated with the binding of GFP and mCh are concentrated inside the nanopore relative to the membrane surface. Two factors contribute to this observation: First of all, confinement effects result in a greater effective concentration of the receptor inside the nanopore and thus enhance binding of the analyte relative to the surface of the membrane. Second, the ion track etching procedure generates additional COOH groups that can

be functionalized with Nbs inside the nanopore. Combined, these effects account for the high responsiveness of the nanopore sensors that are capable of resolving analyte concentrations well below the experimentally determined K_Ds observed in solution.

Methodologically, the approach features a number of unique technical developments. First, Nbs can be directly conjugated to the COOH-groups on the surface of track-etched nanopores obviating the need for the specialist chemist expertise. This means, the chemical reagents are readily available off-the-shelf while the molecular components can be recombinantly produced and tailored in *E. coli* obviating the need for additional functionalization with chemical polymers. In addition, a capacity to express Nbs in *E. coli* greatly facilitate their adaptation and optimization to the functional requirements of a nanopore sensor. Second, taking advantage of the defined 3D structure of proteins, the assembly and immobilization of receptors can be achieved in a directed and controlled fashion. In contrast, conventional immobilization methods based on non-covalent electrostatic interactions[10] or reactions between surface accessible lysine residues with activated *N*-hydroxysuccinimide esters[11] only provide little control how a fusion protein is immobilized. In particular, immobilization may turn out heterogenous with detrimental effects on the performance of a biosensor especially when the binding site of receptor is occluded. Third, the system is highly modular as one can readily adapt the approach to alternative receptor proteins by exchanging the fusion partner of the SpyCatcher.

With an elementary approach established, future studies can now focus on the systematic functionalization of track-etched nanopore membranes drawing on the rich functional repertoire of natural and artificially engineered proteins. This includes both fundamental studies looking to examine how confining proteins inside track-etched nanopores affect their responsiveness toward an analyte in the context of different nanopores while developing them toward distinct applications in biomedical diagnostics or environmental monitoring. The latter will also require the development of standardized manufacturing methods as statistical quantifications across independently manufactured single pore membranes is currently limited by their unique profile. Notably, variability in the manufacturing process arises from the distribution of kinetic energies of the ion beam used to generate latent tracks, the lack of standardized procedures to etch nanopores, which depends on a significant amount of manual handling steps, and, finally, the semi-crystalline nature of the membrane that features both amorphous and crystalline areas. In the future, these limitations can be overcome by applying the methodological framework developed in this study in the context of commercial multipore membranes or membranes for which standardized manufacturing processes have been established, for instance, based on anodized aluminium oxide that feature comparable geometries to track etched conical nanopores.[34]

4. Experimental Section

Materials: Irradiated PET membranes were obtained from the GSI Helmholtz Center for Heavy Ion Research in Darmstadt, Germany. Chemicals (NaOH for track-etching nanopores, KCl for *I–V* measurements, and DBCO and Azp for surface conjugation with proteins) were sourced commercially (Sigma Aldrich). Commercial PBS solution (Carl Roth) was used and composed of 137 mM NaCl, 2.7 mM KCl, 10 mM Na_2HPO_4, and 2.0 mM KH_2PO_4 pH 7.4. The DNA coding for the different protein components (SpyTag002-tether, SpyCatcher002, Nb^{GFP}, Nb^{mCh}, $Nb^{\alpha Amy}$, GFP, and mCh) was purchased commercially (gBlock DNA fragments; Integrated DNA Technologies). An enhanced version of the SpyCatcher, termed SpyCatcher002,[28] was used to immobilize Nbs inside track-etched nanopores. Constructs were cloned into suitable expression vectors for recombinant protein production in *E. coli* either on their own or as a fusion protein by means of the iFLinkC DNA assembly process.[35] The complete amino acid sequences of individual expression constructs are outlined in the Supporting Information. Porcine pancreatic α-Amy was purchased commercially (Catalogue no. **A6255**, Sigma Aldrich).

Recombinant Protein Expression and Purification: Proteins were generally expressed in *E. coli* BL21(DE3) under the control of an IPTG-inducible T7 promoter and purified by Strep-tag affinity chromatography. Detailed protocols on the expression, purification, and functionalization of individual proteins are provided in the Supporting Information. Functionalization of the SpyTag tether with an azide-group was performed according to established protocols.[26] TEV protease for proteolytic processing of the MBP-SpyTag tether was produced according to established protocols.[36] All recombinantly expressed, purified, and modified proteins were finally buffered in PBS before being applied to the membrane.

Nanopore Fabrication: Conical nanopores were fabricated in two steps: Briefly, PET foils (Hostaphan RN12 purchased by Hoechst-Germany) with a thickness of 12 µm were first irradiated with swift heavy ions (Au^{26+}, E_{kin} = 11.4 MeV) at the Universal Linear Accelerator (UNILAC) located at the GSI Helmholtz Center for Heavy Ion Research in Darmstadt, Germany. To this end, membranes featuring single and multiple latent tracks could be generated depending on the fluency of the ion beam.[37] Latent ion tracks were then transformed into conical nanopores through the asymmetric etching technique. To this end, the membrane was fixed between two custom-made conductivitiy cells, and the chemical etching process initiated from the *cis* side (cone base) using 9 M NaOH and stopped with 1 M KCl and 1 M formic acid on the *trans* side (cone tip).[38] Alternatively, to prepare cylindrical nanopores for CLSM studies, multipore membranes were dipped into 2 M NaOH at 50 °C for a fixed period of time according to previously published protocols.[39]

Functional Modification of Track-Etched PET Membranes: Nanopores were functionalized via the COOH-groups that were generated following hydrolysis of PET esters during the track etching process and exposure of the PET surface to NaOH. The COOH-groups were first activated with carbodiimide and subsequently modified with 100 µM DBCO using a standard peptide coupling protocol.[40] Following reaction, the chambers were washed and rinsed four times with PBS pH 7.4. Then, a 20 nM solution of azide-modified SpyTag-tether (in PBS buffer pH 7.4) was added to the membrane and left to react with the cyclooctyene-moiety of DBCO for 6 h at 37 °C. Following reaction, the chambers were washed and rinsed four times with PBS pH 7.4. Finally, a 30 µM solution of SpyCatcher-Nanobody (in PBS buffer pH 7.4) was added and left to react with the SpyTag-Tether for 6 h at 37 °C.[27] Note, during the entire modification process, the nanopore foil remained fixed between the two compartments of the conductivity cell. Reagents were generally added from both sides of the membrane.

Optical Characterization of Functionalized Track-Etched Nanopores: CLSM measurements were performed using a LEICA TCS SP8 (Leica Microsystems, Mannheim, Germany) equipped with a HC PL APO CS2 63 × /1.20 water objective. For imaging, foils with a nanopore density of 10^7 nanopores per cm² were fixed on coverslips using a thin agarose film (0.5% agarose in deionized water) with the tip side facing the agarose. GFP and mCh were then added to the base side and incubated for 30 min until they were drawn via the nanopores into the agarose bed. Afterward the foils were washed twice with PBS to remove any unbound protein. Images were taken with a 488 nm laser for GFP (5% laser power; em. range of 510—525 nm; gain 190 V hybrid detector; scan

speed 400 Hz; line average 4x) and a 561 nm laser for mCh (10% laser power; em. range 600–620 nm; gain 332 V hybrid detector; scan speed 400 Hz; line average 4×). Please note, different parameters for excitation and detection are necessitated by the different photophysical properties of sfGFP (extinction coefficient: 83 300 M^{-1} cm^{-1}; quantum yield: 0.65; brightness: 54.15) and mCh (extinction coefficient: 72 000 M^{-1} cm^{-1}; quantum yield: 0.22; brightness: 15.84).[41] Analysis of the images was performed with Fiji-ImageJ.[42]

Electrical Recordings of Functionalized Track-Etched Nanopores: The modification and functional properties of track-etched single conical nanopores were analyzed by recording the *I–V* characteristics of functionalized membranes. Measurements were generally performed at 25 °C according to published protocols.[43] Briefly, the membrane was mounted between the two half-chambers of the conductivity cell filled with the electrolyte solution (1× PBS buffer pH 7.4 supplemented with an additional 100 mM KCl). Furthermore, a pair of Ag/AgCl electrodes connected to a picoammeter/voltage source (Keithley 6487, Keithley instruments, Ohio) were placed in each chamber solution. The positive pole faced the tip side while the negative pole was oriented toward the bulk side of the nanpore. Afterward, the measurement set up was placed in a faraday cage and grounded. To record *I–V* curves, a scanning triangular voltage was applied from –1 to 1 V using Labview 6.1 (National Instruments) and the transmembrane current was recorded. *I–V* measurements were performed before and after each modification step. Upon treatment of functionalized nanopores with the different analytes GFP, mCh, and α-Amy, the electrolyte solution was composed of the PBS-buffered KCl-solution and a specific amount of analyte. During the entire modification and sensing process, the nanopore remained fixed between both conductivity cells. This ensured the comparability of the nanopore before and after surface functionalization, and following treatment with different analytes while the chambers were repeatedly washed four times and rinsed with PBS pH 7.4.

Supporting Information

Supporting Information is available from the Wiley Online Library or from the author.

Acknowledgements

I.D. and A.G. contributed equally to this work. The authors would like to thank Vanessa Mehlhorn for her assistance with data acquisition. The authors thank Prof. Christiane Trautmann and Dr. Maria E. Toimil Molares from GSI Darmstadt for providing irradiated polymer membranes. The heavy ion irradiation was based on a UMAT experiment, which was performed at the X0-beamline of the UNILAC at the GSI Helmholtzzentrum fuer Schwerionenforschung, Darmstadt (Germany) in the frame of FAIR Phase-0. LOEWE iNAPO, Hessen State Ministry of Higher Education, Research and the Arts (VS, WE, AT), Liebig Fellowship of the Fonds der Chemischen Industrie im Verband der Chemischen Industrie e.V. (AT), the Athene Young Investigator Program (AT), and the Knut and Alice Wallenberg Foundation and Wallenberg Centre of Molecular and Translational Medicine (AT) are gratefully acknowledged.

Open access funding enabled and organized by Projekt DEAL.

Conflict of Interest

The authors declare no conflict of interest.

Data Availability Statement

The data that support the findings of this study are available from the corresponding author upon reasonable request.

Keywords

biosensors, current rectification, molecular diagnostics, nanobodies, nanofluidic devices, synthetic nanopores, track-etched membrane

Received: February 22, 2021
Revised: April 17, 2021
Published online: July 3, 2021

[1] B. Derkus, *Biosens. Bioelectron.* **2016**, *79*, 901.
[2] G. Maduraiveeran, M. Sasidharan, V. Ganesan, *Biosens. Bioelectron.* **2018**, *103*, 113.
[3] T. Ma, J. M. Janot, S. Balme, *Small Methods* **2020**, *4*, 2000366.
[4] D. Kaya, K. Keçeci, *J. Electrochem. Soc.* **2020**, *167*, 037543.
[5] L. K. Müller, I. Duznovic, D. Tietze, W. Weber, M. Ali, V. Stein, W. Ensinger, A. A. Tietze, *Chem. - Eur. J.* **2020**, *26*, 8511.
[6] M. Ali, P. Ramirez, I. Duznovic, S. Nasir, S. Mafe, W. Ensinger, *Colloids Surf., B* **2017**, *150*, 201.
[7] M. Ali, S. Nasir, P. Ramirez, J. Cervera, S. Mafe, W. Ensinger, *J. Phys. Chem. C* **2013**, *117*, 18234.
[8] J. Wang, J. Hou, H. Zhang, Y. Tian, L. Jiang, *ACS Appl. Mater. Interfaces* **2018**, *10*, 2033.
[9] M. Ali, S. Nasir, W. Ensinger, *Chem. Commun.* **2015**, *51*, 3454.
[10] W. Khalid, M. A. Abbasi, M. Ali, Z. Ali, M. Atif, C. Trautmann, W. Ensinger, *Electrochim. Acta* **2020**, *337*, 135810.
[11] M. Bernhard, M. Diefenbach, M. Biesalski, B. Laube, *ACS Sens.* **2020**, *5*, 234.
[12] M. Ali, R. Neumann, W. Ensinger, *ACS Nano* **2010**, *4*, 7267.
[13] M. Ali, B. Yameen, R. Neumann, W. Ensinger, W. Knoll, O. Azzaroni, *J. Am. Chem. Soc.* **2008**, *130*, 16351.
[14] M. Lepoitevin, M. Bechelany, E. Balanzat, J. M. Janot, S. Balme, *Electrochim. Acta* **2016**, *211*, 611.
[15] M. Lepoitevin, T. Ma, M. Bechelany, J. M. Janot, S. Balme, *Adv. Colloid Interface Sci.* **2017**, *250*, 195.
[16] A. Bouchet-Spinelli, E. Descamps, J. Liu, A. Ismail, P. Pham, F. Chatelain, T. Leichlé, L. Leroy, P. Noel Marche, C. Raillon, A. Roget, Y. Roupioz, N. Sojic, A. Buhot, V. Haguet, T. Livache, P. Mailley, *Biosensors* **2019**, *9*, 121.
[17] S. Muyldermans, *Annu. Rev. Biochem.* **2013**, *82*, 775.
[18] C. S. Bever, J. X. Dong, N. Vasylieva, B. Barnych, Y. Cui, Z. L. Xu, B. D. Hammock, S. J. Gee, *Anal. Bioanal. Chem.* **2016**, *408*, 5985.
[19] A. Kirchhofer, J. Helma, K. Schmidthals, C. Frauer, S. Cui, A. Karcher, M. Pellis, S. Muyldermans, C. S. Casas-Delucchi, M. C. Cardoso, H. Leonhardt, K.-P. P. Hopfner, U. Rothbauer, *Nat. Struct. Mol. Biol.* **2010**, *17*, 133.
[20] P. C. Fridy, Y. Li, S. Keegan, M. K. Thompson, I. Nudelman, J. F. Scheid, M. Oeffinger, M. C. Nussenzweig, D. Fenyö, B. T. Chait, M. P. Rout, *Nat. Methods* **2014**, *11*, 1253.
[21] A. Desmyter, S. Spinelli, F. Payan, M. Lauwereys, L. Wyns, S. Muyldermans, C. Cambillau, *J. Biol. Chem.* **2002**, *277*, 23645.
[22] N. Pishesha, J. R. Ingram, H. L. Ploegh, *Annu. Rev. Cell Dev. Biol.* **2018**, *34*, 163.
[23] I. Chen, B. M. Dorr, D. R. Liu, *Proc. Natl. Acad. Sci. U. S. A.* **2011**, *2011*, 11399.
[24] S. C. Reddington, M. Howarth, *Curr. Opin. Chem. Biol.* **2015**, *29*, 94.
[25] P. Y. Apel, Y. E. Korchev, Z. Siwy, R. Spohr, M. Yoshida, *Nucl. Instrum. Methods Phys. Res., Sect. B* **2001**, *184*, 337.
[26] J. E. Glasgow, M. L. Salit, J. R. Cochran, *J. Am. Chem. Soc.* **2016**, *138*, 7496.
[27] B. Zakeri, J. O. Fierer, E. Celik, E. C. Chittock, U. Schwarz-Linek, V. T. Moy, M. Howarth, *Proc. Natl. Acad. Sci. U. S. A.* **2012**, *109*, E690.

[28] A. H. Keeble, A. Banerjee, M. P. Ferla, S. C. Reddington, I. N. A. K. Anuar, M. Howarth, *Angew. Chem., Int. Ed.* **2017**, *56*, 16521.
[29] G. Rompianesi, A. Hann, O. Komolafe, S. P. Pereira, B. R. Davidson, K. S. Gurusamy, *Cochrane Database Syst. Rev.* **2017**, *21*, CD012010.
[30] K. J. Freedman, S. R. Haq, J. B. Edel, P. Jemth, M. J. Kim, *Sci. Rep.* **2013**, *3*, 1638.
[31] K. J. Freedman, M. Jürgens, A. Prabhu, C. W. Ahn, P. Jemth, J. B. Edel, M. J. Kim, *Anal. Chem.* **2011**, *83*, 5137.
[32] D. S. Talaga, J. Li, *J. Am. Chem. Soc.* **2009**, *131*, 9287.
[33] H. Zhang, Y. Tian, L. Jiang, *Nano Today* **2016**, *11*, 61.
[34] H. Robatjazi, S. M. Bahauddin, L. H. Macfarlan, S. Fu, I. Thomann, *Chem. Mater.* **2016**, *28*, 4546.
[35] A. Gräwe, J. Ranglack, A. Weyrich, V. Stein, *Nucleic Acids Res.* **2020**, *28*, e24.
[36] R. B. Kapust, J. Tözsér, J. D. Fox, D. E. Anderson, S. Cherry, T. D. Copeland, D. S. Waugh, *Protein Eng., Des. Sel.* **2001**, *14*, 993.
[37] Z. Siwy, A. Fuliński, *Phys. Rev. Lett.* **2002**, *89*, 198103.
[38] Z. Siwy, P. Apel, D. Dobrev, R. Neumann, R. Spohr, C. Trautmann, K. Voss, *Nucl. Instrum. Methods Phys. Res., Sect. B* **2003**, *208*, 143.
[39] Q. H. Nguyen, M. Ali, V. Bayer, R. Neumann, W. Ensinger, *Nanotechnology* **2010**, *21*, 365701.
[40] M. Ali, P. Ramirez, S. Mafé, R. Neumann, W. Ensinger, *ACS Nano* **2009**, *3*, 603.
[41] T. J. Lambert, *Nat. Methods* **2019**, *16*, 277.
[42] C. T. Rueden, J. Schindelin, M. C. Hiner, B. E. DeZonia, A. E. Walter, E. T. Arena, K. W. Eliceiri, *BMC Bioinformatics* **2017**, *18*, 529.
[43] M. Ali, V. Bayer, B. Schiedt, R. Neumann, W. Ensinger, *Nanotechnology* **2008**, *19*, 485711.

